

# Study of in vitro RBCs membrane elasticity with AOD scanning optical tweezers

HUADONG SONG, YING LIU,\* BIN ZHANG, KANGZHEN TIAN, PANPAN ZHU, HAO LU, AND QI TANG

Jiangsu Key Laboratory of Advanced Laser Materials and Devices, College of Physics & Electronic Engineering, Jiangsu Normal University, Xuzhou, Jiangsu, China

\*liuying70@126.com

**Abstract:** The elasticity of red cell membrane is a critical physiological index for the activity of RBC. Study of the inherent mechanism for RBCs membrane elasticity transformation is attention-getting all along. This paper proposes an optimized measurement method of erythrocytes membrane shear modulus incorporating acousto-optic deflector (AOD) scanning optical tweezers system. By use of this method, both membrane shear moduli and sizes of RBCs with different in vitro times were determined. The experimental results reveal that the RBCs membrane elasticity and size decline with in vitro time extension. In addition, semi quantitative measurements of S-nitrosothiol content in blood using fluorescent spectrometry during in vitro storage show that RBCs membrane elasticity change is positively associated with the S-nitrosylation level of blood. The analysis considered that the diminished activity of the nitric oxide synthase makes the S-nitrosylation of in vitro blood weaker gradually. The main reason for worse elasticity of the in vitro RBCs is that S-nitrosylation effect of spectrin fades. These results will provide a guideline for further study of in vitro cells activity and other clinical applications.

© 2016 Optical Society of America

**OCIS codes:** (000.1430) Biology and medicine; (350.4855) Optical tweezers or optical manipulation.

## References and links

1. N. Hamasaki and M. Yamamoto, "Red blood cell function and blood storage," *Vox Sang.* **79**(4), 191–197 (2000).
2. M. Whirter, J. Liam, H. Noguchi, and G. Gompper, "Ordering and arrangement of deformed red blood cells in flow through microcapillaries," *New J. Phys.* **14**(8), 6709–6717 (2012).
3. M. Musielak, "Red blood cell-deformability measurement: review of techniques," *Clin. Hemorheol. Microcirc.* **42**(1), 47–64 (2009).
4. S. Svetina, G. Kokot, T. S. Kebe, B. Žekš, and R. E. Waugh, "A novel strain energy relationship for red blood cell membrane skeleton based on spectrin stiffness and its application to micropipette deformation," *Biomech. Model. Mechanobiol.* **15**(3), 745–758 (2016).
5. G. J. Streekstra, J. G. G. Dobbe, and A. G. Hoekstra, "Quantification of the fraction poorly deformable red blood cells using ektacytometry," *Opt. Express* **18**(13), 14173–14182 (2010).
6. L. Dintenfass, "Internal viscosity of the red cell and a blood viscosity equation," *Nature* **219**(5157), 956–958 (1968).
7. H. L. Reid, A. J. Barnes, P. J. Lock, J. A. Dormandy, and T. L. Dormandy, "A simple method for measuring erythrocyte deformability," *J. Clin. Pathol.* **29**(9), 855–858 (1976).
8. A. Ashkin, J. M. Dziedzic, J. E. Bjorkholm, and S. Chu, "Observation of a single-beam gradient force optical trap for dielectric particles," *Opt. Lett.* **11**(5), 288–290 (1986).
9. S. Hénon, G. Lenormand, A. Richert, and F. Gallet, "A new determination of the shear modulus of the human erythrocyte membrane using optical tweezers," *Biophys. J.* **76**(2), 1145–1151 (1999).
10. S. Suresh, J. P. Mills, A. Micoulet, M. Dao, C. T. Lim, M. Beil, and T. Seufferlein, "Connections between single-cell biomechanics and human disease states: gastrointestinal cancer and malaria," *Acta Biomater.* **1**(1), 15–30 (2005).
11. M. M. Brandão, A. Fontes, M. L. Barjas-Castro, L. C. Barbosa, F. F. Costa, C. L. Cesar, and S. T. Saad, "Optical tweezers for measuring red blood cell elasticity: application to the study of drug response in sickle cell disease," *Eur. J. Haematol.* **70**(4), 207–211 (2003).
12. R. Agrawal, T. Smart, J. N. Cardoso, C. Richards, R. Bhatnagar, A. Tufail, D. Shima, P. H. Jones, and C. Pavesio, "Assessment of red blood cell deformability in type 2 diabetes mellitus and diabetic retinopathy by dual optical tweezers stretching technique," *Sci. Rep.* **6**, 15873 (2016).

13. J. Sleep, D. Wilson, R. Simmons, and W. Gratzner, "Elasticity of the red cell membrane and its relation to hemolytic disorders: an optical tweezers study," *Biophys. J.* **77**(6), 3085–3095 (1999).
14. Y. Tan, D. Sun, J. Wang, and W. Huang, "Mechanical characterization of human red blood cells under different osmotic conditions by robotic manipulation with optical tweezers," *IEEE Trans. Biomed. Eng.* **57**(7), 1816–1825 (2010).
15. Y. Li, C. Wen, H. Xie, A. Ye, and Y. Yin, "Mechanical property analysis of stored red blood cell using optical tweezers," *Colloids Surf. B Biointerfaces* **70**(2), 169–173 (2009).
16. C. T. Lim, M. Dao, S. Suresh, C. H. Sow, and K. T. Chew, "Large deformation of living cells using laser traps," *Acta Mater.* **52**(7), 1837–1845 (2004).
17. M. Dao, C. T. Lim, and S. Suresh, "Mechanics of the human red blood cell deformed by optical tweezers," *J. Mech. Phys. Solids* **51**(11–12), 2259–2280 (2003).
18. M. Dao, J. Li, and S. Suresh, "Molecularly based analysis of deformation of spectrin network and human erythrocyte," *Mater. Sci. Eng. C* **26**(8), 1232–1244 (2006).
19. H. Felgner, O. Müller, and M. Schliwa, "Calibration of light forces in optical tweezers," *Appl. Opt.* **34**(6), 977–982 (1995).
20. Y. Q. Chen, C. W. Chen, Y. L. Ni, Y. S. Huang, O. Lin, S. Chien, L. A. Sung, and A. Chiou, "Effect of N-ethylmaleimide, chymotrypsin, and H<sub>2</sub>O<sub>2</sub> on the viscoelasticity of human erythrocytes: experimental measurement and theoretical analysis," *J. Biophotonics* **7**(8), 647–655 (2014).
21. M. Grau, S. Pauly, J. Ali, K. Walpurgis, M. Thevis, W. Bloch, and F. Suhr, "RBC-NOS-dependent S-nitrosylation of cytoskeletal proteins improves RBC deformability," *PLoS One* **8**(2), e56759 (2013).
22. E. L. Florin, A. Pralle, E. H. K. Stelzer, and J. K. H. Hörber, "Photonic force microscope calibration by thermal noise analysis," *Appl. Phys., A Mater. Sci. Process.* **66**(7), S75–S78 (1998).
23. M. M. Haque, M. G. Moisesescu, S. Valkai, A. Dér, and T. Savopol, "Stretching of red blood cells using an electro-optics trap," *Biomed. Opt. Express* **6**(1), 118–123 (2015).
24. S. Fusco, P. Memmolo, L. Miccio, F. Merola, M. Mugnano, A. Paciello, P. Ferraro, and P. A. Netti, "Nanomechanics of a fibroblast suspended using point-like anchors reveal cytoskeleton formation," *RSC Advances* **6**(29), 24245–24249 (2016).
25. H. Zhang and K. K. Liu, "Optical tweezers for single cells," *J. R. Soc. Interface* **5**(24), 671–690 (2008).
26. S. M. Block, "Optical tweezers: A new tool for biophysics," in *Noninvasive Techniques in Cell Biology*, S. Grinstein, K. Foskett, ed. (Wiley, 1990).
27. L. Miccio, P. Memmolo, F. Merola, S. Fusco, V. Embrione, A. Paciello, M. Ventre, P. A. Netti, and P. Ferraro, "Particle tracking by full-field complex wavefront subtraction in digital holography microscopy," *Lab Chip* **14**(6), 1129–1134 (2014).
28. C. Veigel and C. F. Schmidt, "Moving into the cell: single-molecule studies of molecular motors in complex environments," *Nat. Rev. Mol. Cell Biol.* **12**(3), 163–176 (2011).
29. A. van der Horst and N. R. Forde, "Calibration of dynamic holographic optical tweezers for force measurements on biomaterials," *Opt. Express* **16**(25), 20987–21003 (2008).
30. A. Ashkin, "Forces of a single-beam gradient laser trap on a dielectric sphere in the ray optics regime," *Biophys. J.* **61**(2), 569–582 (1992).
31. K. H. Parker and C. P. Winlove, "The deformation of spherical vesicles with permeable, constant-area membranes: application to the red blood cell," *Biophys. J.* **77**(6), 3096–3107 (1999).
32. M. Keshive, S. Singh, J. S. Wishnok, S. R. Tannenbaum, and W. M. Deen, "Kinetics of S-nitrosation of thiols in nitric oxide solutions," *Chem. Res. Toxicol.* **9**(6), 988–993 (1996).
33. D. R. Arnette and J. S. Stamler, "NO<sup>+</sup>, NO, and NO<sup>-</sup> donation by S-nitrosothiols: implications for regulation of physiological functions by S-nitrosylation and acceleration of disulfide formation," *Arch. Biochem. Biophys.* **318**(2), 279–285 (1995).
34. P. S. Y. Wong, J. Hyun, J. M. Fukuto, F. N. Shirota, E. G. DeMaster, D. W. Shoeman, and H. T. Nagasawa, "Reaction between S-nitrosothiols and thiols: generation of nitroxyl (HNO) and subsequent chemistry," *Biochemistry* **37**(16), 5362–5371 (1998).
35. D. Giustarini, A. Milzani, I. Dalle-Donne, and R. Rossi, "Detection of S-nitrosothiols in biological fluids: a comparison among the most widely applied methodologies," *J. Chromatogr. B Analyt. Technol. Biomed. Life Sci.* **851**(1–2), 124–139 (2007).
36. P. Damiani and G. Burini, "Fluorometric determination of nitrite," *Talanta* **33**(8), 649–652 (1986).
37. Z. Peng, X. Li, I. V. Pivkin, M. Dao, G. E. Karniadakis, and S. Suresh, "Lipid bilayer and cytoskeletal interactions in a red blood cell," *Proc. Natl. Acad. Sci. U.S.A.* **110**(33), 13356–13361 (2013).
38. M. Grau, P. Friederichs, S. Krehan, C. Koliomitra, F. Suhr, and W. Bloch, "Decrease in red blood cell deformability is associated with a reduction in RBC-NOS activation during storage," *Clin. Hemorheol. Microcirc.* **60**(2), 215–229 (2015).

## 1. Introduction

Red blood cells (RBCs) are responsible for delivering oxygen to tissues and organs mainly. The past studies have discovered that the character change of normal RBC will cause harm to human life [1]. So RBCs play a key role in our health. In the human microcirculation system, RBCs need sufficient deformability to pass through the capillaries which are smaller than

their diameter [2]. Obviously the elasticity is significant to RBCs activity. Therefore the detection technologies of RBCs elasticity are indispensable in biomedical research [3]. The early measurement technologies include micropipette aspiration [4], ektacytometry [5], viscometry [6], micropore filtration [7] and etc. These methods are greatly developed and widely applied. However, most of them merely can characterize the colonial elasticity of RBCs. Even the membrane shear modulus as an important physical parameter for describing the RBCs elasticity couldn't be measured precisely for a long time in the past. But innovation is endless. A paper about single beam gradient force trap marked the beginning of optical tweezers technology development [8]. Soon afterwards the optical tweezers were employed extensively as an effective tool to investigate the cell and biomacromolecule. In sum, Optical tweezers have many advantages in biomechanics research, such as single cell level operation, high accuracy and little damage to biological tissue. Since Sylvie Hénon et al measured the shear modulus of single RBC membrane successfully with double optical tweezers [9], plenty of researchers have shifted their sights to study deformability of RBCs with optical tweezers. The recent main research contents include the following several aspects: (1) The influences of sickle cell disease, malaria, diabetes and other blood diseases on RBCs deformation and drug treatment of pathological RBCs [10–13]; (2) The transformation of RBCs deformation under different physiological environments [14, 15]; (3) The analysis of RBCs deformation by combining optical tweezers with the finite element simulation [16–18].

For the former studies, there are some imperfections. In terms of optical tweezers method for measuring RBCs membrane shear modulus. Although researchers presented different measurement procedures, few people have optimized them. It's noticeable that the experimental efficiency relies on the sample pretreatment process and the operation complexity of optical tweezers. Through comparing these measurement procedures, we have recognized that double-beads adhesion strategy is superior to other methods due to higher precision and relative controllable adhesion area between the bead and the cell [9, 11, 15]. In previous reports, some researchers use the modified micro beads as handles to attach the RBCs that cost too much time [14, 15]. Certainly the effects of functional modification reagents on the experiment are unknown as well as. Alternatively the nonspecific adhesion of silica micro beads can be used to realize the double ball adhesion of RBCs at diameter direction. In addition, Mostly researchers tended to pull one RBC with different forces via repeatedly changing laser power. The more flexible method is to estimate the real-time drag force by means of trap stiffness calibration before measurement [19]. Meanwhile, previous measurement procedures need experimenters to manipulate the specimen stage manually because of optical tweezers setup limitation. Some multi-trap optical tweezers such as acousto-optic deflector (AOD) scanning optical tweezers are more convenient than manually-operated one. According to above discusses, the improvement of measurement method based on previous experience is necessary.

Besides, the researches of the relation between the chemical compositions and the deformability of RBCs have been reported rarely [20]. Further study focused on this point can expand our knowledge about the inherent mechanism of RBCs deformability. Recently, researchers found that there is a connection between the S-nitrosylation and RBCs deformability [21]. The reported experiment assessed the resulting influence of changing the nitric oxide synthase activity on in vitro RBCs deformability. Unfortunately the experimental methodology is indirect. It can't reflect the real change relation between the S-nitrosylation levels and the in vitro RBCs elasticity. So we desire to explore the detail to a certain extent.

In this letter, we implement an optimized measurement method of erythrocyte membrane elasticity via employing the AOD scanning optical tweezers system which provides an efficiency operation, and combining with a simple sample preparation process that omitted the modification of micro beads. The variation trends of elasticity and sizes of in vitro RBCs stored at 4 °C were obtained. Further measurements of S-nitrosothiol content of blood using

fluorescent spectrometry during in vitro storage were utilized to confirm the relation between the S-nitrosylation level of blood and RBCs membrane elasticity change.

## 2. Experimental setup and method

### 2.1 Experiment setup

The AOD scanning optical tweezers system (Tweez250si) was purchased from Aresis Company. The key components consist of a 5000mW Nd:YAG laser source (1064 nm) connected to a 60 × water immersion inverted microscope (Nikon Eclipse Ti), highly sensitive CMOS camera (PL-B74 IU) and AOD, as shown in Fig. 1. Profiting from the AOD, the optical trap position and strength can be arbitrarily controlled just by cursor based on computer soft (Trap positioning resolution is < 0.001 nm). The experimental images are captured by CMOS camera and recorded by the computer in real time. The recorded data are subsequently analyzed by image analysis software (TweezForce) ships with the system. Handily we can calibrate optical trap stiffness by thermal noise analysis [22], then figure out the real-time force throughout the experiment.

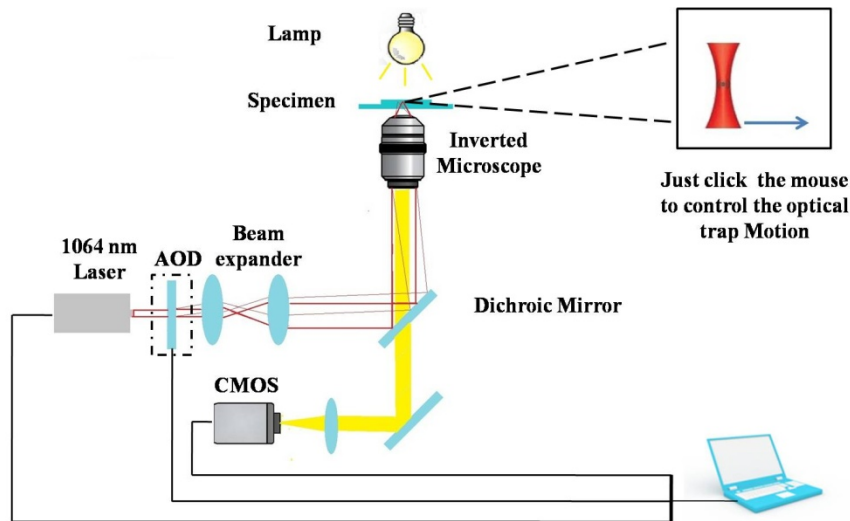


Fig. 1. The schematic diagram of AOD scanning optical tweezers system. A continuous wave laser beam emitted by Nd:YAG laser pass through the AOD controlled by computer to achieve beam shifting. Then the beam is expanded by beam expander before it is transmitted into the microscope. The expanded beam is coupled into the optical pathway of the microscope by a Dichroic Mirror after which it is tightly focused into the sample chamber using a water immersion objective lens with Numerical Aperture (NA) of 1.0. The experimental images are captured by CMOS camera.

### 2.2 Experiment sample preparation

The blood used in experiments was extracted from a healthy donor and stored at 4 °C. Silicon beads with 4 μm in diameter were selected as the handles. The RBCs and micro beads were washed separately and mixed together in the phosphate-buffered saline (PBS) (HyClone SH30256.01B, pH 7.2) with the bead-cell concentration ratio of 2:1. Through the several washing processes, contaminant on the micro beads was removed. The non-specific adhesion between the RBCs and micro beads can therefore be ensured in the cell-bead incubation process. After 40 min incubation at 4 °C, the mixed suspension was diluted and dropped into sample cell. A small amount of bovine serum albumin (BSA) (Sigma A 4503) was coated on the bottom to prevent RBCs from sticking on the glass plate of the sample cell. By the way,

we didn't need to worry about the elasticity aberrance of RBCs due to artificial variation in the value of pH. Because the pH value of buffer solution was identical to normal blood.

### 2.3 Measurement method

The first step in the measurement was to stretch the RBC. The cell stretching technologies are emerging inexhaustibly as well as [23–25]. Considering the intuitiveness and easiness, our stretching method is shown in Fig. 2. Two micro beads are adhered to RBC diametrically. We could observe plenty of cell-bead connectors that meet this measurement standard in sample cell, due to large incubation amount. When stretching the red cell, one bead was stayed adhering to the bottom of sample cell with non-specific adhesion, and the other was trapped and dragged by optical trap in predefined path. The dragged velocity controlled by computer was smaller than  $0.02 \mu\text{m/s}$ , so the viscous drag force could be ignored. The continuous stretching video of every RBC was recorded and remained to be analyzed. The real-time pull force can be calculated according to the shift between the center of the micro bead and the optical trap after calibrating optical trap stiffness. All observations and measurements were made at room temperature ( $25^\circ\text{C}$ ) in the laboratory. The temperature increase due to trapping a particle in water has been roughly estimated to be rather low [26]. So we could assume that the temperature of the sample was  $25^\circ\text{C}$  at the time of measurement.

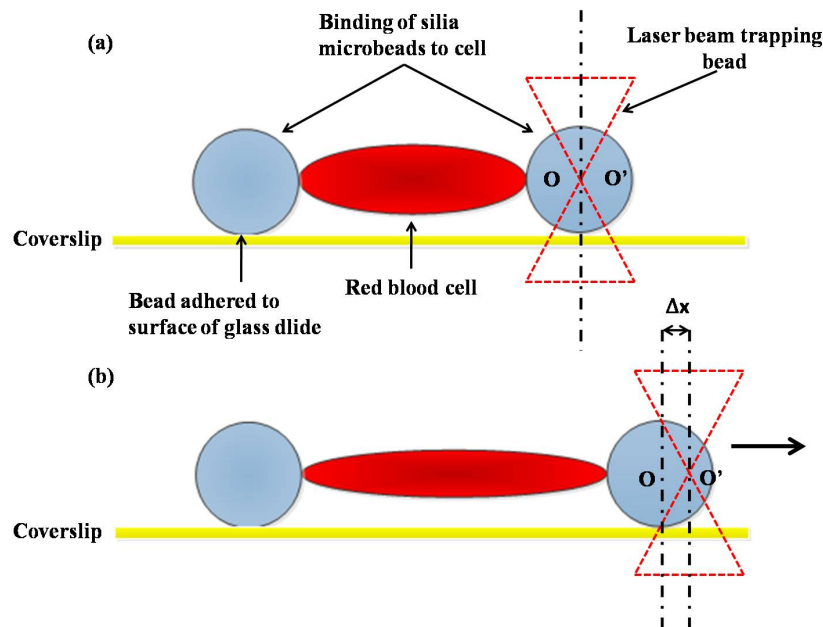


Fig. 2. Schematic drawings for RBC stretched by laser tweezers. (a) Before stretching; (b) After stretching. The continuous stretching video of RBC will be recorded. The real-time pull force can be calculated according to the shift between the center of the micro bead and the optical trap.

This experimental method draws lessons from the previous advantage procedures in sample preparation and simplifies the process for double-beads adhesion of RBC. Furthermore, we employ the advantages of AOD scanning optical tweezers to reduce the operation of specimen platform. It decreases the measurement time greatly. The experiment proved that it is easily operational and practicable.

### 2.4 Calibration of optical trap stiffness

In the experiment, the pull force for stretching RBC was identified on the basis of its relation with the optical trap stiffness. In comparison, the thermal noise analysis is simpler among all



calibration methods of trap stiffness [27–29]. Near the center of the optical trap, the force exerted on the trapped micro bead (silica bead or polystyrene bead) is proportional to the offset of the micro bead relative to the optical trap center:

$$F = -k_x \cdot \Delta x, \quad (1)$$

in which  $k_x$  means trapping stiffness,  $F$  is the trap force,  $\Delta x$  is the shift between the center of the micro bead and the optical trap. The potential field near the center of optical trap is harmonic:

$$E(x) = \frac{1}{2} k_x \cdot \Delta x^2. \quad (2)$$

In order to calibrate the trap stiffness with thermal noise analysis, traditionally we trap a micro bead. The micro bead will do random thermal motion nearby the equilibrium spot in the potential field. Its position distribution probability density obeys the Boltzmann statistics [22]:

$$p(x) = c \cdot e^{\frac{-E(x)}{k_B \cdot T}}, \quad (3)$$

$k_B$  is Boltzmann constant,  $T$  is absolute temperature,  $c$  is normalization factor.

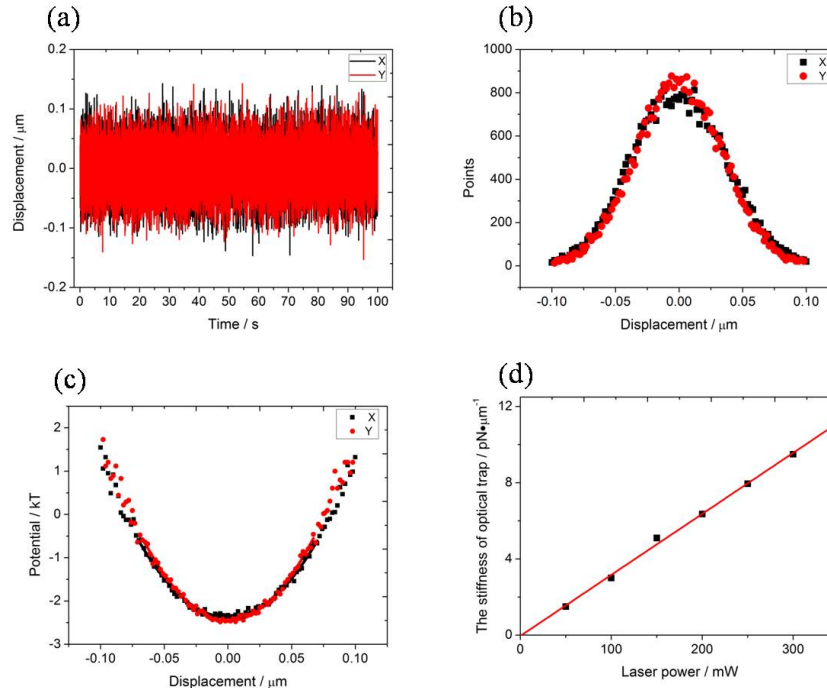


Fig. 3. Optical stiffness Measurement with thermal noise analysis. (a) Brownian motion trajectory of trapped micro bead at laser power  $P = 200$  mW; (b) the probability of the position distribution of the micro bead at laser power  $P = 200$  mW; (c) fitting of optical trap potential at laser power  $P = 200$  mW; (d) calibration curve of the trapping stiffness at different laser power.

Figure 3(a)-3(c) shows the measurement process of optical trap stiffness with laser power of 200 mW. Firstly, the Brownian motion trajectory of the microsphere in an optical trap was captured, and the position distribution probabilities of the microsphere were obtained by the

motion trajectory statistics. Then the distribution of the optical trap potential field was derived using the Eq. (3). The optical trap stiffness was evaluated by fitting the distribution data of the optical trap potential field. Especially the trap stiffnesses under different laser powers are shown in Fig. 3(d). The relationship between optical trap stiffness and laser power is linear, which is consistent with the theoretical calculation [30]. The stiffness corresponding to other laser power can be attained by linear fitting. It is worth paying attention that we had to calibrate the trap stiffness near the glass surface and keep the distance almost constant in the course of the experiment, which caused very little deviation of calibration force when pulling the RBC.

### 3. Results

We measure the stretching of fresher RBCs in vitro (stored for 2 days at 4 °C). In the experiment, the different size RBCs (size in a range from 6.7  $\mu\text{m}$  to 7.7  $\mu\text{m}$ ) were randomly chosen in order to keep the experimental data representative. Figure 4 shows the stretching of RBC under different forces.

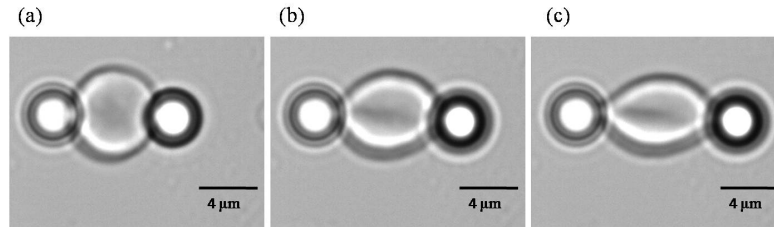


Fig. 4. The stretching of RBC (in vitro time: 2 days) under different forces: (a) 0 pN; (b) 2.5 pN; (c) 5 pN.

Through video Analysis and data preparation, the relationship scatter diagrams between optical trap forces (the drag force exerted on the RBCs) and RBCs extension ratio were acquired and shown in Fig. 5. We get the slope  $k$  from the fitting results of these scatter diagrams. The shear moduli of RBCs were calculated by putting the slope  $k$  substitute into the following expression [31]:

$$H = \sqrt{\frac{1}{125k^3 \cdot d \cdot B}}, \quad (4)$$

in which,  $d$  is the diameter of RBCs, the bending modulus  $B = 2 \times 10^{-19} \text{ N} \cdot \text{m}$ .

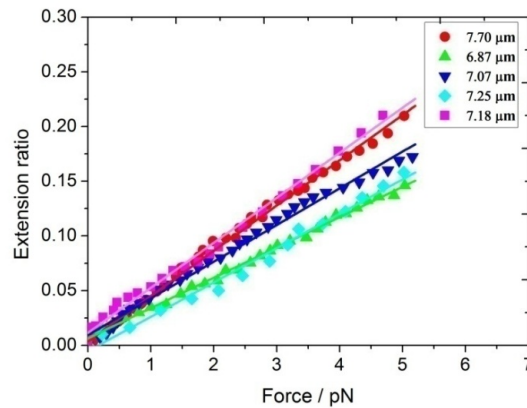


Fig. 5. Extension ratio-Force relation curves of RBCs and fitting lines (in vitro time: 2 days).

The slope values in Fig. 5 are 0.0448, 0.0433, 0.03, 0.036 and 0.031 separately. Correspondingly, the shear moduli of different size RBCs are  $7.61 \mu\text{N/m}$ ,  $8.48 \mu\text{N/m}$ ,  $14.48 \mu\text{N/m}$ ,  $10.86 \mu\text{N/m}$  and  $13.43 \mu\text{N/m}$ . The fresh RBC shear modulus is  $10.95 \pm 2.67 \mu\text{N/m}$ .

Moreover, we measure the change of the RBCs membrane elasticity with different in vitro times. At least 5 cells were used every time. The extension ratio-Force relation curves of RBCs with different in vitro times are shown in Fig. 6.

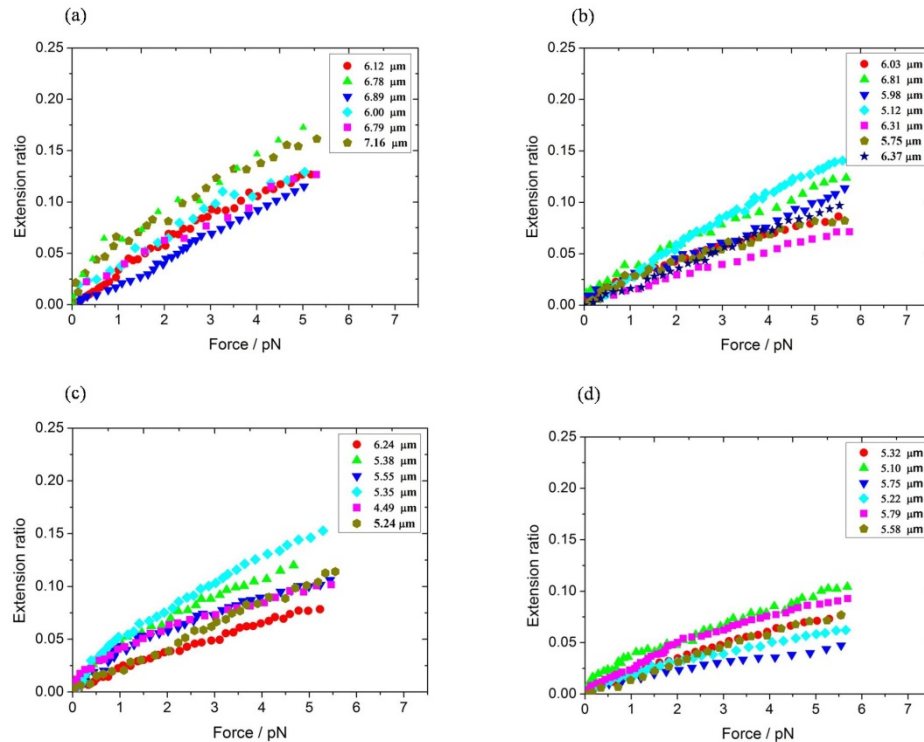


Fig. 6. Extension ratio-Force relationship diagrams of RBCs with different in vitro days. (a) 6 days, (b) 10 days, (c) 14 days and (d) 18 days.

Similarly, we obtain the membrane shear moduli of in vitro RBCs stored for 6 days, 10 days, 14 days and 18 days are  $17.77 \pm 3.13 \mu\text{N/m}$ ,  $41.44 \pm 14.63 \mu\text{N/m}$ ,  $59.56 \pm 21.18 \mu\text{N/m}$  and  $78.65 \pm 15.91 \mu\text{N/m}$  separately. The variation tendency is shown in Fig. 7(a). The RBCs membranes shear moduli increase along with in vitro time extension. So the elasticity of RBCs becomes worse gradually. At same time, the red cells size variation is shown in Fig. 7(b). The figure shows that the RBCs size becomes smaller and keeps unchanged up to 18 days. We must emphasize that the size of RBC can't be used to reflect the membrane elasticity indirectly, though it looks like that the increase in membrane shear moduli and the decrease in sizes of the RBCs are inversely related. The shear modulus is the most intrinsic parameter to characterize the elasticity of RBC membrane. The size is just an auxiliary characterization for the RBC membrane loss. According to our experimental data, the elasticity of a small size RBC may be greater than the big size one, under same in vitro time. It's distinct that the shear modulus calculation Eq. (4) is related not only with the diameter of RBCs, but also with the extension ratio-Force relation curve slope of RBC.



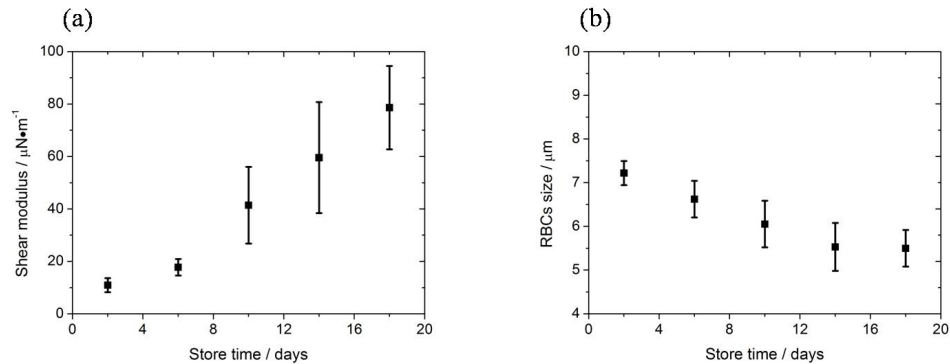
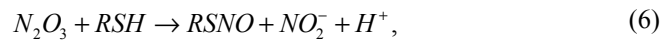


Fig. 7. Variation tendency of the membrane shear moduli and the RBCs size.

According to the former reports, RBCs deformability is related to the protein S-nitrosylation. The protein S-nitrosylation process is expressed in the following chemical formula [32–34]:



in which, RSH represents the free sulfhydryl protein, RSNO is S-nitrosothiol. In order to investigate the relation between the protein S-nitrosylation level of blood and RBCs membrane elasticity change, this paper complete the semi quantitative measurements of S-nitrosothiol content of blood based on fluorescent spectrometry during in vitro storage [35, 36]. The measurement method can be found in literature [35]. In the experiment,  $\text{CuCl}_2$  solution was used as the splitting agent to make RSNOs release NO that was equivalent to the RSNOs. NO reacts with oxygen to produce NOx. 2, 3-diaminonaphthalene (DAN) which was used as the fluorescent probe to react with NOx to produce the strong fluorescent substance 2, 3-naphthotriazole (DAT):



The fluorescence intensity of DAT can represent the concentration of RSNOs in blood indirectly, so the measurement is Semi quantitative. The amount of blood measured was 200  $\mu\text{l}$  every time. 2 ml 300  $\mu\text{mol/L}$  solution of DAN (MACKLIN D807411) in PBS was added. The complete reaction needed 2 hours. Then the fluorescence spectrum was detected by FS920 spectrofluorometer (Edinburgh Instruments). An excited light with 383 nm in wavelength was adopted. The fluorescence spectrum of DAT derived from the reaction of DAN and RSNOs in different in vitro blood are shown in Fig. 8(a). Emission peak intensity at 408 nm was used as the characterization of RSNOs content according to previous report [36]. Figure 8(b) shows the change curve of peak intensity at 408 nm as a function of in vitro times. It reveals that the content of RSNOs in blood is decreasing until remaining unchanged during in vitro time. In other words, S-nitrosylation level weakened. By comparison with Fig. 7(a), we found that RBCs membrane elasticity change is positively associated with the S-nitrosylation level of blood.

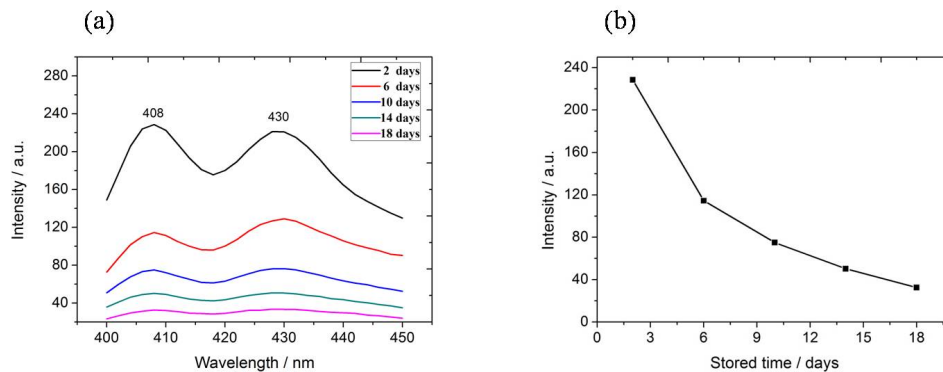


Fig. 8. (a) the fluorescence spectrum of DAT that source from the reaction of DAN and RSNOs in different in vitro stored blood; (b) the change curve of DAT fluorescence peak intensity at 408 nm during storage.

#### 4. Discussion

The red cell membrane consists of two components: a lipid bilayer and a 2D spectrin network that known as the membrane skeleton [37], as shown in Fig. 9. The spectrin is attached to the internal surface of lipid bilayer by means of connected Actin, anchor protein, transmembrane protein and etc. The spectrin network contributes to the elasticity and shape of RBC.

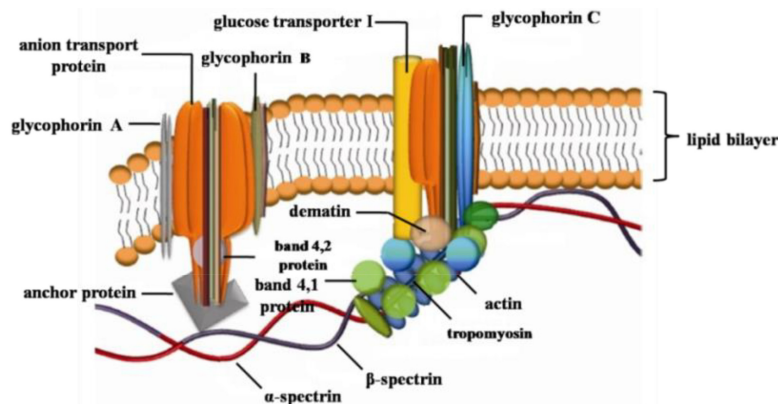


Fig. 9. The composition of RBC membrane.

Studies have shown that the S-nitrosylation of protein is an important process of protein function regulation. The effect of the S-nitrosylation on the function of RBCs membrane skeleton is no exception. In the blood, NO is produced by the conversion of L-arginine to L-citrulline mediated by the activity of the nitric oxide synthase (NOS). During blood storage the NOS activity will decrease [38], which results in the decline of NO. Naturally, the S-nitrosylation effect fades. Our experimental results proved it. So the spectrin with low S-nitrosylation level will lose control function of RBC membrane elasticity and shape gradually. Thus the RBCs membrane shear moduli become increasingly greater.

#### 5. Summary

The paper realized the rapid measurement of RBCs membrane elasticity through optimizing the experimental method based on AOD scanning optical tweezers, and studied the connection between the S-nitrosylation of blood and RBCs deformability. It all comes down to here:

- (1) According to experimental data, the in vitro RBCs membrane shear moduli increase along with stored time extended. The elasticity of RBCs becomes worse and worse. At same time, it was found that the cell size decreased with the increase of the in vitro storage time, until keeping constant.
- (2) Semi quantitative measurements of S-nitrosothiol content of blood show that the S-nitrosylation level of blood is depressed.
- (3) The analysis shows that the S-nitrosylation of spectrin weakened, and then the spectrin's ability to maintain elasticity and shape of red blood cell decreased.

The relationship between RBCs deformation and the S-nitrosylation of spectrin will gives us a deeper understanding about the mechanism of RBCs membrane elasticity change.

### **Funding**

National Natural Science Foundation of China (NSFC) (61575087); Natural Science Foundation of Jiangsu Province (BK20151164).

### **Acknowledgments**

Many thanks to Dr. Ying Wu for experimental guide. Some suggestions on paper writing were put forward by Changchun Yan and Caiqin Han.